

# Blue-Light-Emitting Fluorene-Based Polymers with Tunable Electronic Properties

Bin Liu,<sup>†</sup> Wang-Lin Yu,<sup>†</sup> Yee-Hing Lai,<sup>\*,‡</sup> and Wei Huang<sup>\*,†</sup>

*Institute of Materials Research and Engineering (IMRE), National University of Singapore, 3 Research Link, Singapore 117602, Republic of Singapore, and Department of Chemistry, National University of Singapore, 10 Kent Ridge Crescent, Singapore 117543, Republic of Singapore*

Received September 5, 2000. Revised Manuscript Received April 17, 2001

A series of soluble alternating polyfluorene copolymers with different main chain structures and those of the same main chain structure polyfluorene-*co-alt*-phenylene with different functional groups attached at the 2- and/or 5-positions of the phenylene ring were synthesized by a palladium-catalyzed Suzuki coupling reaction. All 10 polymers had the band gaps ranging from 2.81 to 3.35 eV, corresponding to blue-light emission. Through controllable modification for both the main chain structures and the side chains, not only the optical and electronic properties of the blue emissive polymers had been tuned, but also the structure–property relationships, especially the HOMO and LUMO energy level engineering, had been studied. Relatively high PL efficiency in both solution and film states, good thermal stability, and relatively high glass transition temperatures were demonstrated on these polymers. In general, polymers with the main chain structure of polyfluorene-*co-alt*-phenylene were found to have higher  $\Phi_{\text{fl}}$  both in solution and in solid states than those copolymers with other main chain structures. For the polymers with the same main chain structure of polyfluorene-*co-alt*-phenylene, attachment of electron-donating alkoxy groups on phenylene ring (**P4**) had caused a spectral red shift, corresponding to slightly decreased HOMO and increased LUMO energy levels, while attachment of electron-withdrawing ester groups (**P6**) had led to an obvious blue shift in the absorption spectrum with a decrement in both the HOMO and LUMO energy levels as compared to that of the unsubstituted polymer (**P2**). As for the polymers of different main chain structures, in comparison with the homopolymer **P1**, carbazole comonomer had caused an obvious spectral blue shift with increased HOMO and decreased LUMO energy levels. A decrement in both the HOMO and LUMO energy levels had been observed for **P9** in which naphthalene was chosen as the comonomer. However, for **P10**, although there was no obvious difference between the absorption and emission spectra of **P10** as compared to those of **P1**, both the HOMO and LUMO energy levels were reduced greatly when they were compared with those of **P1**.

## Introduction

The wideranging application of electroactive and photoactive conjugated polymers have attracted great interest in the development of conjugated functional polymers. In particular, significant progress has been achieved in the development of light-emitting diodes (LEDs) based on conjugated polymers.<sup>1–3</sup> Important molecular structures for light-emitting applications have been reviewed recently.<sup>2,3</sup> Although all three primary colors (red, green, and blue) required by full color displays have been demonstrated in PLEDs,<sup>2,4</sup> only red

(orange) and green PLEDs have sufficient efficiencies and lifetimes to be of commercial value. Pursuing efficient and stable blue LEDs based on conjugated polymers remains a challenge. The first blue LED has been fabricated from poly(*p*-phenylene) (PPP).<sup>5</sup> Subsequently, polyfluorenes (PFs),<sup>6–8</sup> polycarbazoles (PCs),<sup>9</sup> polythiophene derivatives (PTs),<sup>10–13</sup> derivatives of poly-

\* To whom correspondence should be addressed. Tel.: (65) 874 8592. Fax: (65) 872 0785. E-mail: wei-huang@imre.org.sg.

<sup>†</sup> IMRE, National University of Singapore.

<sup>‡</sup> Department of Chemistry, National University of Singapore.

(1) Greenham, N. C.; Friend, R. H. *Solid State Phys.* **1995**, *49*, 1.  
(2) Kraft, A.; Grimsdale, A. C.; Holmes, A. B. *Angew. Chem., Int. Ed.* **1998**, *37*, 402.

(3) Segura, J. L. *Acta Polym.* **1998**, *49*, 319.

(4) Friend, R. H.; Gymer, R. W.; Holmes, A. B.; Burroughes, J. H.; Marks, R. N.; Taliani, C.; Bradley, D. A.; Santos, D.; Brédas, J. L.; Lögdlund, M.; Salaneck, W. R. *Nature* **1999**, *397*, 121.

(5) Grem, G.; Leditzky, G.; Ulrich, B.; Leising, G. *Adv. Mater.* **1992**, *4*, 36.

(6) Ohmori, Y.; Uchida, M.; Muro, K.; Yoshino, K. *Jpn. J. Appl. Phys.* **1991**, *30*, L1941.

(7) Pei, Q.; Yang, Y. *J. Am. Chem. Soc.* **1996**, *118*, 7416.

(8) Ranger, M.; Rondeau, D.; Leclerc, M. *Macromolecules* **1997**, *30*, 7686.

(9) Kido, J.; Hongawa, K.; Okuyama, K.; Nagai, K. *Appl. Phys. Lett.* **1993**, *63*, 2627.

(10) Berggren, M.; Inganäs, O.; Gustafsson, G.; Rasmusson, J.; Andersson, M. R.; Hjertberg, T.; Wennerstrom, O. *Nature* **1994**, *372*, 444.

(11) Andersson, M. R.; Berggren, M.; Inganäs, O.; Gustafsson, G.; Gustafsson-Carlberg, J. C.; Selse, D.; Hjertberg, T.; Wennerstrom, O. *Macromolecules* **1995**, *28*, 7525.

(12) Granström, M.; Inganäs, O. *Appl. Phys. Lett.* **1996**, *68*, 147.

(13) Andersson, M. R.; Thomas, O.; Mammo, W.; Svensson, M.; Theander, M.; Inganäs, O. *J. Mater. Chem.* **1999**, *9*, 1933.

paraphenylene with ladder structures,<sup>14,15</sup> and some copolymers based on fluorene<sup>16,17</sup> or pyridine<sup>18</sup> have also been introduced as blue-emissive polymers. In recent years, polyfluorene derivatives have aroused special interest because of their high efficiencies both in photoluminescence (PL) and in electroluminescence (EL).<sup>19–21</sup>

The electronic properties of a conjugated polymer is primarily governed by the chemical structure of the backbone itself; a number of additional tools have also been employed to further adjust the HOMO and LUMO energy levels of the conjugated polymers.<sup>1,22–25</sup> For most of the PFs investigated so far, their relatively large band gaps and especially the high-energy barriers for hole injection have limited their applications in PLEDs.<sup>20,26</sup> It is well-known that the balanced charge injection from both electrodes and the comparable mobility of electrons and holes within the polymers are crucial for achieving high device efficiency. Several strategies, such as introducing hole injection and/or a hole-transporting layer to balance the injection of the two types of electrical charges, have been established to improve the EL efficiencies of PLEDs, including blue PLEDs.<sup>27–30</sup> Alternatively, a more attractive way to achieve high efficiency in PLEDs is to develop new conjugated polymers with the desired injection ability for electrons and/or holes. To succeed, it is essential to find an effective synthetic methodology to adjust the HOMO and LUMO energy levels of the conjugated polymers. In this respect, however, because of the lesser amount of freedom of chemical modification compared to other backbone-structured conjugated polymers, for PFs, the only available possibility of remote functionalization is at the C-9 position; any other position of the fluorene unit is difficult for performing conventional chemical modifications.

The copolymerization approach has been widely used in the preparation of conjugated polymers to achieve specific electronic and physical properties. It is also demonstrated that copolymerization of fluorene with

various aryl partners allows for tunability of electronic properties with enhanced stability.<sup>17,31</sup> In this article, we will present a new series of fluorene-based alternating copolymers. By copolymerization with different aryl comonomers, the electronic properties of the resultant polymers are tuned in a wide range, while the blue emission is well maintained. Moreover, comonomers provide the opportunity of bonding different functional side chain groups so that the electronic and physical properties of the polymers may be further tunable. The structure–property relationships within the blue alternating copolymers are also studied.

## Experimental Section

**General.** Chemicals and reagents were purchased from Aldrich Chemical Co. unless otherwise stated. All new compounds were characterized by <sup>1</sup>H NMR, <sup>13</sup>C NMR, and elemental analyses. NMR spectra were collected on a Bruker ACF 300 spectrometer with chloroform-*d* as the solvent and tetramethylsilane as the internal standard. Melting points (mp) were measured with an Electrothermal IA 9300 digital melting-point apparatus. Thermogravimetric analyses (TGA) were conducted on a Du Pont Thermal Analyst 2100 system with a TGA 2950 thermogravimetric analyzer under a heating rate of 20 °C/min and a nitrogen flow rate of 70 mL/min. Differential scanning calorimetry (DSC) was run on a Du Pont DSC 2910 module in conjunction with the Du Pont Thermal Analyst system at a heating rate of 20 °C/min. Elemental microanalyses were carried out by the Microanalysis Lab of the National University of Singapore. UV–vis spectra were recorded on a Shimadzu 3101 spectrophotometer. Fluorescence measurement was carried out on a Perkin-Elmer LS 50B luminescence spectrometer with a xenon lamp as a light source. Cyclic voltammetry (CV) was performed on an EG&G Parc model 273A potentiostat/galvanostat system with a three-electrode cell in a solution of Bu<sub>4</sub>NClO<sub>4</sub> (0.10 M) in acetonitrile at a scan rate of 50 mV/s. GPC analysis was conducted with a Waters 2690 separation module equipped with a Waters 410 differential refractometer HPLC system and Waters Styragel HR 4E columns using polystyrene as the standard and THF as the eluant.

**Synthesis.** 2,7-Dibromo-9,9-dihexylfluorene (**1**),<sup>8</sup> 2,5-dibromo-1,4-dihexylbenzene (**3**),<sup>32</sup> 2,5-dibromo-1,4-dihexyloxybenzene (**4**),<sup>33</sup> and 3,4-didecylthiophene<sup>34</sup> were prepared following the literature procedures. 1,4-Dibromobenzene (**2**) and 2,5-dibromopyridine (**10**) were obtained from Aldrich Chemical Co. and used without further purification.

**2,5-Dibromobenzonitrile (5).**<sup>35</sup> Bromine (22.4 g, 140 mmol) was added dropwise to a mixture of benzonitrile (5.0 g, 48 mmol) and aluminum chloride (21.0 g, 150 mmol) at room temperature. The mixture was heated at 60 °C for 6 h and then at 120 °C for 12 h. After it cooled to room temperature, the mixture was poured into ice water. The product was extracted with ether and the combined organic extracts were washed with aqueous sodium thiosulfate and dried over anhydrous magnesium sulfate. The solvent was removed in vacuo to give a light brown solid. Twice recrystallization from benzene afforded **5** as colorless crystals (4.8 g, 39%). mp 141–142 °C. <sup>1</sup>H NMR (CDCl<sub>3</sub>, 300 MHz, ppm) δ 7.82 (m, 1H), 7.64 (m, 1H), 7.55 (m, 1H). Anal. Calcd for C<sub>7</sub>H<sub>3</sub>NBr<sub>2</sub>: C, 32.22; H, 1.16; N, 5.37; Br, 61.25. Found: C, 32.21; H, 1.21; N, 5.69; Br, 61.06.

(14) Grüner, J.; Hamer, P. J.; Friend, R. H.; Huber, H. J.; Scherf, U.; Holmes, A. B. *Adv. Mater.* **1994**, *6*, 748.

(15) Stampfl, J.; Tarch, S.; Leising, G.; Scherf, U. *Synth. Met.* **1995**, *71*, 2125.

(16) Cho, H. N.; Kim, D. Y.; Kim, Y. C.; Lee, J. Y.; Kim, C. Y. *Adv. Mater.* **1997**, *9*, 326.

(17) Kreyenschmidt, H.; Kaerner, G.; Fuhrer, T.; Ashenurst, J.; Karg, S.; Chen, W. D.; Lee, V. Y.; Scott, J. C.; Miller, R. D. *Macromolecules* **1998**, *31*, 1099.

(18) Wang, H. L.; Park, J. W.; Fu, D. K.; Marsella, M. J.; Swager, T. M.; MacDermid, A. G.; Wang, Y. Z.; Gebler, D. G.; Epstein, A. J. *Polym Prepr.* **1995**, *36*, 45.

(19) Grice, A. W.; Bradley, D. D. C.; Bernius, M. T.; Indasekaran, M.; Wu, W. W.; Woo, E. P. *Appl. Phys. Lett.* **1998**, *73*, 629.

(20) Janietz, S.; Bradley, D. D. C.; Grell, M.; Giebeler, C.; Inbasekaran, M.; Woo, E. P. *Appl. Phys. Lett.* **1998**, *73*, 2453.

(21) Klaerner, G.; Miller, R. D. *Macromolecules* **1998**, *31*, 2007.

(22) Xu, B.; Holderoft, S. *Macromolecules* **1993**, *26*, 4457.

(23) Hay, M.; Klavetter, F. L. *J. Am. Chem. Soc.* **1995**, *117*, 7112.

(24) Brédas, J. L. *Adv. Mater.* **1995**, *7*, 263.

(25) Moratti, S. C.; Cervini, R.; Holmes, A. B.; Baigent, D. R.; Friend, R. H.; Greenham, N. C.; Grüner, J.; Hamer, P. J. *Synth. Met.* **1995**, *71*, 2117.

(26) Kim, J. S.; Friend, R. H.; Cacialli, F. *Appl. Phys. Lett.* **1999**, *74*, 3084.

(27) Yu, W. L.; Cao, Y.; Pei, J.; Huang, W.; Heeger, A. J. *Appl. Phys. Lett.* **1999**, *75*, 3270.

(28) Campbell, A. J.; Bradley, D. D. C.; Antoniadis, H.; Inbasekaran, M.; Wu, W. S.; Woo, E. P. *Appl. Phys. Lett.* **2000**, *76*, 1734.

(29) Sainova, D.; Miteva, T.; Nothofer, H. G.; Scherf, U.; Glowacki, I.; Ulanski, J.; Fujikawa, H.; Neher, D. *Appl. Phys. Lett.* **2000**, *76*, 1810.

(30) Jiang, X. Z.; Liu, S.; Ma, H.; Jen, A. K. Y. *Appl. Phys. Lett.* **2000**, *76*, 1813.

(31) Klärner, G.; Davey, M. H.; Chen, W. D.; Scott, J. C.; Miller, R. D. *Adv. Mater.* **1998**, *10*, 993.

(32) Miyaura, N.; Suzuki, A. *Chem. Rev.* **1995**, *95*, 2457.

(33) Ruiz, J. P.; Dharra, J. R.; Reynolds, J. R. *Macromolecules* **1992**, *25*, 849.

(34) Destri, S.; Pasini, M.; Pelizzi, C.; Porzio, W.; Predieri, G.; Vignali, C. *Macromolecules* **1999**, *32*, 353.

(35) Hird, M.; Gray, G. W.; Toyne, K. J. *Mol. Cryst. Liq. Cryst.* **1991**, *206*, 205.

**Diethyl-2,5-dibromoterephthalate (6).**<sup>36</sup> To a mixture of 2,5-dibromo-*p*-xylene (13.2 g, 50 mmol) and sodium hydroxide (18.0 g, 450 mmol) in 350 mL of water, potassium permanganate (35.0 g, 222 mmol) was added, and the mixture was heated to reflux for 12 h. Upon cooling, the black precipitate was filtered off and the filtrate was acidified with concentrated HCl to give crude 2,5-dibromoterephthalic acid (4.8 g, 30%). The crude acid was put into 50 mL of absolute ethanol with 2 mL of concentrated sulfuric acid, and the resulting mixture was heated to reflux for another 24 h. The solvent was removed under reduced pressure, and the residue was purified by column flushing with hexane and ethyl acetate to afford **6** (2.1 g, 40%) as a white solid. mp 126–127 °C. <sup>1</sup>H NMR (CDCl<sub>3</sub>, 300 MHz, ppm) δ 8.22 (s, 2H), 4.44–4.36 (q, 4H, *J* = 7.09 Hz), 1.43–1.37 (t, 6H, *J* = 7.20 Hz). Anal. Calcd for C<sub>12</sub>H<sub>12</sub>O<sub>4</sub>Br<sub>2</sub>: C, 37.89; H, 3.16; Br, 42.11. Found: C, 37.88; H, 2.36; Br, 42.30.

**2,5-Dibromo-3,4-didecylthiophene (7).**<sup>37</sup> A solution of NBS (4.4 g, 25 mmol) in 20 mL of DMF was slowly added dropwise to a solution of 3,4-didecylthiophene (3.6 g, 10 mmol) in 20 mL of DMF, which is exclusive of light, and the mixture was stirred overnight. It was poured into ice and extracted several times with ether. The combined organic phase was washed with water and then dried over magnesium sulfate. Evaporation of the solvent and purification by column flushing with hexane as the eluant afforded **7** (4.2 g, 80%) as a colorless oil. <sup>1</sup>H NMR (CDCl<sub>3</sub>, 300 MHz, ppm) δ 2.52–2.47 (t, 4H, *J* = 7.83 Hz), 1.45–1.40 (m, 4H), 1.33–1.20 (m, 28H), 0.89–0.85 (t, 6H, *J* = 6.42 Hz). Anal. Calcd for C<sub>24</sub>H<sub>42</sub>Br<sub>2</sub>S: C, 55.17; H, 8.10; Br, 30.59, S, 6.14. Found: C, 55.07; H, 8.07; Br, 28.38; S, 5.76.

**3,6-Dibromo-N-(2-ethylhexyl)carbazole (8).**<sup>38</sup> To a solution of 3,6-dibromocarbazole (6.5 g, 20 mmol) dissolved in 50 mL of anhydrous DMF was added potassium carbonate (5.5 g, 40 mmol). The mixture was allowed to stir for 1 h, after which 2-ethylhexylbromide (5.8 g, 30 mmol) was added dropwise. The reaction was allowed to reflux for 2 days. After it cooled, the mixture was poured into water and extracted with chloroform three times and the combined organic layer was dried over anhydrous magnesium sulfate. The solvent and the unreacted 2-ethylhexylbromide were removed under reduced pressure and the residue was purified by column flushing with hexane and ethyl acetate to afford **8** (7.0 g, 80%) as a waxy solid. mp 62–63 °C. <sup>1</sup>H NMR (CDCl<sub>3</sub>, 300 MHz, ppm) δ 8.17 (s, 2H), 7.60–7.52 (d, 2H, *J* = 8.40 Hz), 7.30–7.23 (d, 2H, *J* = 8.39 Hz), 4.15–4.09 (d, 2H, *J* = 7.65 Hz), 2.01–1.97 (m, 1H, *J* = 6.00 Hz), 1.35–1.25 (m, 8H), 0.96–0.85 (m, 6H). Anal. Calcd for C<sub>20</sub>H<sub>23</sub>NBr<sub>2</sub>: C, 54.92; H, 5.26; N, 3.20; Br, 36.61. Found: C, 54.88; H, 5.06; N, 3.18; Br, 36.50.

**1,4-Dibromonaphthalene (9).**<sup>39</sup> Bromine (102.0 g, 640 mmol) was added slowly to 1,4-dioxane (60.0 g, 630 mmol) in a 500-mL round bottle flask; an exothermic reaction was observed. After addition, solid was afforded and the warm solid was taken up in 1000 mL of ice water. The orange solid was sucked and collected for further use without purification. A solution of the solid (24.8 g, 50 mmol) in 20 mL of 1,4-dioxane was added dropwise to naphthalene (6.4 g, 50 mmol) in 50 mL of 1,4-dioxane. The mixture was allowed to react overnight and then neutralized with 10% sodium hydroxide. The white crystalline residue was purified by recrystallization from absolute ethanol to afford **9** (4.6 g, 32%) as white crystals. mp 81–82 °C. <sup>1</sup>H NMR (CDCl<sub>3</sub>, 300 MHz, ppm) δ 8.27–8.22 (d of d, 2H, *J* = 6.3 and 3.3 Hz), 7.67 (s, 2H), 7.69 (d of d, 2H, *J* = 6.3 and 3.3 Hz), 7.64 (s, 2H). <sup>13</sup>C NMR (CDCl<sub>3</sub>, 75 MHz, ppm) δ 132.8, 129.6, 127.9, 127.5, 122.4. Anal. Calcd for C<sub>10</sub>H<sub>6</sub>Br<sub>2</sub>: C, 42.00; H, 2.11; Br, 55.88. Found: C, 41.85; H, 2.61; Br, 55.29.

**9,9-Dihexylfluorene-2,7-bis(trimethylene boronate) (11).**<sup>40</sup> A solution of 2,7-dibromo-9,9-dihexylfluorene (16.3 g, 33 mmol)

in THF was added slowly with stirring to a mixture of magnesium turnings (1.9 g, 80 mmol) and THF under argon. The Grignard reagent solution was slowly dropped into a stirred solution of trimethyl borate (38 mL, 330 mmol) in THF at –78 °C for 2 h and then at room temperature for 2 days. The reaction mixture was poured into crushed ice containing sulfuric acid (5%) while stirring. The mixture was extracted with ether and the combined extracts were evaporated to give a white solid. Recrystallization of the crude acid from hexane–acetone (1:2) afforded pure 9,9-dihexylfluorene-2,7-diboronic acid (6.3 g, 44%) as white crystals. The diboronic acid (6.3 g, 15 mmol) was then refluxed with 1,3-propanediol (2.0 g, 33 mmol) in toluene for 10 h. After the usual workup, the crude product was recrystallized from hexane to afford **11** (5.5 g, 73%) as white crystals. mp 123–124 °C. <sup>1</sup>H NMR (CDCl<sub>3</sub>, 300 MHz, ppm) δ 7.77 (d, 2H, *J* = 7.55 Hz), 7.72 (s, 2H), 7.69 (d, 2H, *J* = 7.48 Hz), 4.25–4.16 (t, 8H, *J* = 5.36 Hz), 2.07 (m, 4H, *J* = 5.33 Hz), 1.98 (m, 4H, *J* = 4.09 Hz), 1.20–0.90 (m, 12H), 0.76 (t, 6H, *J* = 6.83 Hz), 0.56 (m, 4H). <sup>13</sup>C NMR (CDCl<sub>3</sub>, 75 MHz, ppm) δ 151.17, 140.03, 139.18, 132.44, 128.10, 123.53, 119.83, 109.94, 55.09, 40.28, 31.53, 31.43, 30.82, 29.62, 29.04, 28.71, 23.76, 22.48, 13.94, 13.88. Anal. Calcd for C<sub>31</sub>H<sub>44</sub>O<sub>4</sub>B<sub>2</sub>: C, 74.13; H, 8.83. Found: C, 74.02; H, 8.35.

**Polymerization. General Procedure of Polymerization through the Suzuki Reaction.** To a mixture of 9,9-dihexylfluorene-2,7-bis(trimethylene boronate) (1 equiv), dibromo compound (1 equiv), and tetrakis(triphenylphosphine)palladium [Pd(PPh<sub>3</sub>)<sub>4</sub>] (1.0 mol %) was added a degassed mixture of toluene ([monomer] = 0.25 M) and aqueous 2 M potassium carbonate (3:2 in volume). The mixture was vigorously stirred at 85–90 °C for 48 h. After the mixture was cooled to room temperature, it was poured into 200 mL of the mixture of methanol and deionized water (10:1). A fibrous solid was obtained by filtration. The solid was washed with methanol, water, and then methanol. After washing for 24 h in a Soxhlet apparatus with acetone to remove oligomers and catalyst residues, the resulting polymers were collected and dried under vacuum. Yields: 50–85%.

**Poly(9,9-dihexylfluorene) (P1).** Light yellow powder (yield: 75%). <sup>1</sup>H NMR (CDCl<sub>3</sub>, 300 MHz, ppm) δ 7.84–7.69 (m, 6H), 2.12 (br, 4H), 1.15–0.80 (m, 22H). <sup>13</sup>C NMR (CDCl<sub>3</sub>, 75 MHz, ppm) δ 151.71, 140.42, 139.98, 126.15, 121.40, 119.98, 55.21, 40.23, 31.36, 29.56, 23.74, 22.44, 13.90. Anal. Calcd for C<sub>25</sub>H<sub>32</sub>: C, 90.36; H, 9.64. Found: C, 88.15; H, 9.93.

**Poly[2,7-(9,9-dihexylfluorene)-co-alt-p-phenylene] (P2).** White fibrous solid (yield: 82%). <sup>1</sup>H NMR (CDCl<sub>3</sub>, 300 MHz, ppm) δ 7.82–7.65 (m, 8H), 7.23 (br, 2H), 2.07 (br, 4H), 1.10–0.75 (m, 22H). <sup>13</sup>C NMR (CDCl<sub>3</sub>, 75 MHz, ppm) δ 151.71, 145.48, 140.41, 140.06, 139.55, 127.49, 125.85, 121.37, 120.01, 55.22, 31.40, 29.65, 25.18, 22.51, 16.29, 13.93. Anal. Calcd for C<sub>31</sub>H<sub>36</sub>: C, 91.18; H, 8.82. Found: C, 91.00; H, 8.95.

**Poly[2,7-(9,9-dihexylfluorene)-co-alt-2,5-dihexyl-p-phenylene] (P3).** White powder (yield: 55%). <sup>1</sup>H NMR (CDCl<sub>3</sub>, 300 MHz, ppm) δ 7.84–7.77 (br, 2H), 7.49–7.15 (m, 6H), 2.70 (br, 4H), 2.04 (br, 4H), 1.56 (br, 4H), 1.23–0.84 (m, 40H). <sup>13</sup>C NMR (CDCl<sub>3</sub>, 75 MHz, ppm) δ 150.55, 141.20, 140.58, 139.53, 137.61, 130.99, 127.87, 123.96, 119.21, 55.03, 40.51, 32.98, 31.53, 29.75, 29.35, 23.89, 22.49, 13.91. Anal. Calcd for C<sub>43</sub>H<sub>60</sub>: C, 89.52; H, 10.48. Found: C, 89.47; H, 10.31.

**Poly[2,7-(9,9-dihexylfluorene)-co-alt-2,5-dihexyloxy-p-phenylene] (P4).** White fibrous solid (yield: 85%). <sup>1</sup>H NMR (CDCl<sub>3</sub>, 300 MHz, ppm) δ 7.82–7.79 (d, 2H, *J* = 7.50 Hz), 7.73 (s, 2H), 7.60–7.57 (d, 2H, *J* = 7.81 Hz), 7.14 (s, 2H), 4.01–3.96 (t, 4H, *J* = 6.38 Hz), 2.17 (br, 4H), 1.77–1.72 (m, 4H, *J* = 6.10 Hz), 1.43–0.76 (m, 40H). <sup>13</sup>C NMR (CDCl<sub>3</sub>, 75 MHz, ppm) δ 150.44, 139.80, 137.00, 131.28, 127.90, 124.37, 119.14, 116.77, 69.86, 54.99, 40.52, 31.62, 31.43, 29.90, 29.38, 25.70, 23.94, 22.62, 22.56, 13.90. Anal. Calcd for C<sub>43</sub>H<sub>60</sub>O<sub>2</sub>: C, 84.81; H, 9.93. Found: C, 84.75; H, 9.91.

**Poly[2,7-(9,9-dihexylfluorene)-co-alt-2-cyano-p-phenylene] (P5).** Off-white powder (yield: 65%). <sup>1</sup>H NMR (CDCl<sub>3</sub>, 300 MHz,

(36) Lamba, J. J. S.; Tour, J. M. *J. Am. Chem. Soc.* **1994**, *116*, 11723.

(37) Bäuerle, P.; Pfau, F.; Schlupp, H.; Würthner, F.; Gaudl, K. U.; Caro, M. B.; Fischer, P. *J. Chem. Soc., Perkin Trans 2* **1993**, 489.

(38) Lee, J. H.; Park, J. W.; Choi, S. K. *Synth. Met.* **1997**, *88*, 31.

(39) Lee, S. J. H.; Weber, W. P. *Polym. Bull.* **1989**, *22*, 355.

(40) Yu, W. L.; Pei, J.; Cao Y.; Huang, W.; Heeger, A. J. *Chem. Commun.* **1999**, 1837.



ppm)  $\delta$  8.11–7.63 (m, 9H), 2.12 (br, 4H), 1.25–0.77 (m, 22H).  $^{13}\text{C}$  NMR ( $\text{CDCl}_3$ , 75 MHz, ppm)  $\delta$  152.34, 152.15, 151.81, 151.61, 144.17, 140.94, 140.72, 137.67, 136.84, 132.40, 131.32, 130.52, 127.72, 125.98, 123.40, 121.29, 120.59, 120.28, 118.94, 111.80, 55.63, 40.27, 31.40, 29.59, 23.83, 22.51, 13.89. Anal. Calcd for  $\text{C}_{32}\text{H}_{35}\text{N}$ : C, 88.64; H, 8.14; N, 3.23. Found: C, 87.97; H, 8.08; N, 3.57.

*Poly[2,7-(9,9-dihexylfluorene)-co-alt-2,5-diethylterephthalate]* (**P6**). White fibrous solid (yield: 82%).  $^1\text{H}$  NMR ( $\text{CDCl}_3$ , 300 MHz, ppm)  $\delta$  7.90 (s, 2H), 7.81–7.78 (br, 2H), 7.39 (br, 4H), 4.16–4.09 (q, 4H,  $J = 6.84$  Hz), 2.02 (br, 4H), 1.16–0.77 (m, 28 H).  $^{13}\text{C}$  NMR ( $\text{CDCl}_3$ , 75 MHz, ppm)  $\delta$  168.38, 151.10, 141.15, 140.14, 139.10, 133.77, 131.62, 127.36, 122.88, 119.58, 61.18, 55.29, 40.46, 31.49, 29.71, 23.83, 22.55, 13.86, 12.27. Anal. Calcd for  $\text{C}_{37}\text{H}_{44}\text{O}_4$ : C, 80.40; H, 8.02. Found: C, 80.44; H, 8.12.

*Poly[2,7-(9,9-dihexylfluorene)-co-alt-2,5-(3,4-didecylthiophene)]* (**P7**). Light yellow solid (yield: 79%).  $^1\text{H}$  NMR ( $\text{CDCl}_3$ , 300 MHz, ppm)  $\delta$  7.77–7.75 (br, 2H), 7.50 (br, 4H), 2.71 (br, 4H), 2.04 (br, 4H), 1.57 (br, 4H), 1.32–0.76 (m, 56H).  $^{13}\text{C}$  NMR ( $\text{CDCl}_3$ , 75 MHz, ppm)  $\delta$  150.99, 139.88, 138.86, 137.72, 133.92, 128.15, 123.52, 119.63, 55.10, 31.84, 31.55, 31.11, 29.95, 29.78, 29.56, 29.38, 29.29, 27.92, 23.82, 22.59, 22.56, 14.03, 13.93. Anal. Calcd for  $\text{C}_{49}\text{H}_{74}\text{S}$ : C, 84.41; H, 10.99; S, 4.60. Found: C, 83.76; H, 10.70; S, 4.80.

*Poly[2,7-(9,9-dihexylfluorene)-co-alt-3,6-(N-ethylhexyl)carbazole]* (**P8**). Off-white powder (yield: 54%).  $^1\text{H}$  NMR ( $\text{CDCl}_3$ , 300 MHz, ppm)  $\delta$  8.52 (s, 2H), 7.85–7.52 (m, 10H), 4.28 (br, 2H), 2.17 (br, 4H), 1.48–0.80 (m, 37H).  $^{13}\text{C}$  NMR ( $\text{CDCl}_3$ , 75 MHz, ppm)  $\delta$  151.63, 140.79, 139.49, 132.95, 126.09, 125.43, 123.52, 121.56, 119.75, 118.77, 109.25, 55.28, 40.56, 39.49, 31.43, 31.04, 29.64, 28.85, 24.41, 23.78, 22.94, 22.51, 13.99. Anal. Calcd for  $\text{C}_{45}\text{H}_{55}\text{N}$ : C, 88.67; H, 9.03; N, 2.30. Found: C, 87.69; H, 8.73; N, 2.41.

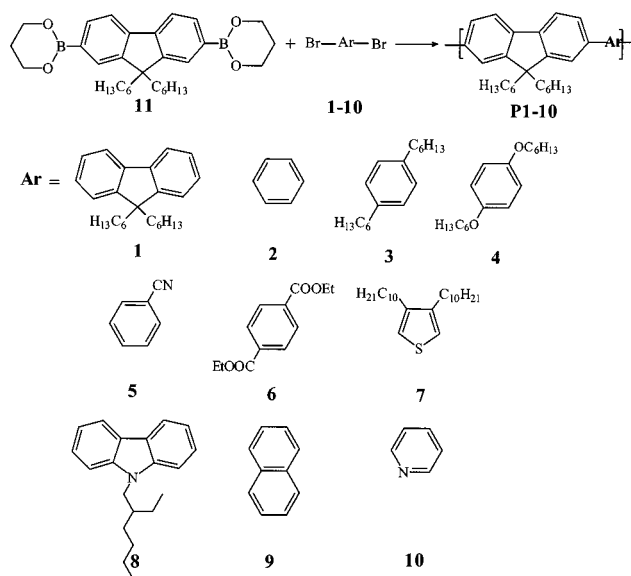
*Poly[2,7-(9,9-dihexylfluorene)-co-alt-1,4-naphthalene]* (**P9**). White powder. (yield: 50%).  $^1\text{H}$  NMR ( $\text{CDCl}_3$ , 300 MHz, ppm)  $\delta$  8.15–7.52 (m, 12H), 2.12 (br, 4H), 1.60–0.85 (m, 22H).  $^{13}\text{C}$  NMR ( $\text{CDCl}_3$ , 75 MHz, ppm)  $\delta$  151.02, 140.28, 140.05, 139.58, 132.22, 128.87, 127.16, 126.49, 125.79, 124.99, 119.67, 55.25, 40.33, 31.52, 29.67, 24.01, 22.53, 13.98. Anal. Calcd for  $\text{C}_{35}\text{H}_{38}$ : C, 91.70; H, 8.29. Found: C, 89.97; H, 8.61.

*Poly[2,7-(9,9-dihexylfluorene)-co-alt-2,5-pyridine]* (**P10**). Light greenish yellow fibrous solid (yield: 85%).  $^1\text{H}$  NMR ( $\text{CDCl}_3$ , 300 MHz, ppm)  $\delta$  9.09 (br, 1H), 8.16–7.60 (m, 8H), 2.13 (br, 4H), 1.11–0.73 (m, 22H).  $^{13}\text{C}$  NMR ( $\text{CDCl}_3$ , 75 MHz, ppm)  $\delta$  155.76, 152.45, 152.15, 151.83, 147.64, 141.75, 140.59, 136.42, 135.31, 128.72, 125.94, 121.29, 120.64, 55.50, 40.33, 31.42, 29.62, 23.82, 22.49, 13.88. Anal. Calcd for  $\text{C}_{30}\text{H}_{35}\text{N}$ : C, 87.97; H, 8.61; N, 3.42. Found: C, 86.93; H, 8.53; N, 3.55.

## Results and Discussion

**Synthesis and Characterization.** The general synthetic route to the polymers is outlined in Scheme 1. 2,5-Dibromo-1,4-dihexyloxybenzene (**4**) was synthesized from hydroquinone through a Williamson ether route in the presence of a strong base, followed by bromination with bromine in tetrachloride with a yield of 85%.<sup>33</sup> 1,4-Dihexylbenzene and 3,4-didecylthiophene were synthesized from 1,4-dibromobenzene and 3,4-dibromothiophene, respectively, through the Grignard coupling reaction with alkylmagnesium bromide catalyzed by [1,3-bis(diphenylphosphino)propane]dichloronickel(II).<sup>32,34</sup> Direct bromination of 1,4-dihexylbenzene with bromine and a small amount of iodine as a catalyzing oxidizing reagent afforded monomer **3** in 50% yield.<sup>32</sup> Bromination of 3,4-didecylthiophene with NBS in DMF afforded the monomer **7** in 85% yield.<sup>37</sup> Monomer **5**, 2,5-dibromobenzonitrile, was prepared in 39%

## Scheme 1. Synthetic Route for the Polymers<sup>a</sup>



<sup>a</sup> Reagents and conditions: (i)  $[(\text{PPh}_3)_4\text{Pd}(0)]$  (1.0 mol %), toluene/2 M  $\text{K}_2\text{CO}_3$  (3:2), reflux.

**Table 1. Molecular Weights and Thermal Analysis Data of P1–P10**

polymer	$M_n$	$M_w$	$M_w/M_n$	$T_g$ (°C)	$T_d$ (°C)
<b>P1</b>	24 300	34 500	1.4	103	390
<b>P2</b>	11 800	20 300	1.7		398
<b>P3</b>	9 400	14 500	1.5	50	390
<b>P4</b>	50 500	100 100	2.0	72	377
<b>P5</b>	22 800	34 600	1.5	123	410
<b>P6</b>	48 100	90 100	1.9	111	331
<b>P7</b>	18 600	29 400	1.6	78	410
<b>P8</b>	8 900	15 600	1.7	145	376
<b>P9</b>	7 300	11 600	1.6	213	390
<b>P10</b>	60 400	118 400	2.0	122	375

yield by a “swamping-catalyst” method<sup>41</sup> (using a large excess of aluminum chloride) in the absence of a solvent.<sup>35</sup> To synthesize monomer **6**, 2,5-dibromo-*p*-xylene was oxidized with potassium permanganate in sodium hydroxide to afford 2,5-dibromoterephthalic acid, which was further esterified to give ethyl-2,5-dibromoterephthalate (**6**) in an overall yield of 12%.<sup>36</sup> 3,6-Dibromo-*N*-(2-ethylhexyl)carbazole (**8**) was obtained with a yield of 80% from 3,6-dibromocarbazole via the nucleophilic substitution with 2-ethylhexylbromide in the solvent DMF, using potassium carbonate as a base.<sup>38</sup> Bromination of naphthalene with a freshly prepared *p*-dioxane bromine complex afforded monomer **9** in a yield of 32%.<sup>39</sup> The monomer **11**, 9,9-dihexylfluorene-2,7-bis(trimethylene boronate), was synthesized using 2,7-dibromofluorene as the starting material.<sup>40</sup> The polymerization depicted in Scheme 1 is based on the Suzuki coupling reaction, which was carried out in a mixture of toluene and aqueous potassium carbonate solution (2 M) containing 1 mol %  $\text{Pd}(\text{PPh}_3)_4$  under vigorous stirring at 85–90 °C for 2 days. All these polymers readily dissolve in common organic solvents, such as chloroform, THF, toluene, and xylene. The number average molecular weights ( $M_n$ ) of the polymers determined by gel permeation chromatography (GPC)

(41) Pearson, D. E.; Stamper, W. E.; Suthers, B. R. *J. Org. Chem.* **1963**, *28*, 3147.

**Table 2. Optical Data and the Fluorescence Quantum Yields (Both in Chloroform Solution and in Film States) of P1–P10**

polymer	solution $\lambda_{\max}$ (nm) <sup>a</sup>		film $\lambda_{\max}$ (nm) <sup>a</sup>		$E_g$ (eV) <sup>b</sup>	PL efficiency (%)	
	abs.	em.	abs.	em.		solution	film
<b>P1</b>	379	415 (438, 469)	385.5	422 (444, 476)	2.86	82.2	73.7
<b>P2</b>	369.5	408 (431.5)	371	422 (441, 470)	2.92	84.5	77.8
<b>P3</b>	326	383 (403)	324	404 (389)	3.32	63.6	87.5
<b>P4</b>	370.5	414 (436)	373.5	418 (414)	2.95	63.1	55.4
<b>P5</b>	366	409.5 (432)	370	423.5 (443)	2.93	73.7	47.9
<b>P6</b>	353	451	350.5	443	3.04	35.1	19.5
<b>P7</b>	367	447 (473)	375.5	458 (478)	2.76	39.6	21.6
<b>P8</b>	348	398 (417)	343	428 (406, 451)	3.06	26.3	10.1
<b>P9</b>	349	418	349	423.5	3.05	58.0	22.6
<b>P10</b>	385	416 (440, 475)	395	426 (447)	2.82	90.5	40.7

<sup>a</sup> The data in the parentheses are the wavelengths of shoulders and subpeaks. <sup>b</sup>  $E_g$  stands for the band gap energy estimated from the onset wavelength of the optical absorption.

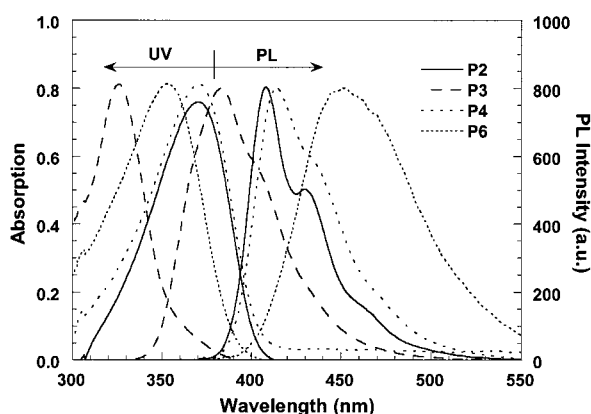


**Figure 1.** UV–visible absorption spectra and photoluminescence spectra of **P2–P4** and **P6** measured from the solutions ( $\approx 1 \times 10^{-5}$  M) in chloroform at room temperature.

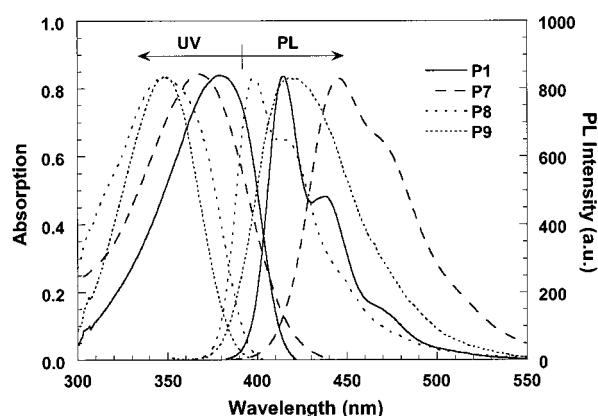


**Figure 2.** UV–visible absorption spectra and photoluminescence spectra of **P1** and **P7–P9** measured from the solutions ( $\approx 1 \times 10^{-5}$  M) in chloroform at room temperature.

were ranging from  $\sim 7300$  to  $\sim 60\,000$  with the polydispersity index of 1.4–2.0 using polystyrene as the standard. (See Table 1.) The chemical structures of the polymers were verified by  $^1\text{H}$  NMR,  $^{13}\text{C}$  NMR, and elemental analyses.

The thermal stability of the polymers in nitrogen was evaluated by thermogravimetric analysis (TGA). The corresponding data are summarized in Table 1. All the polymers (except **P6**, which started weight loss at 331 °C, due to the decomposition of the ester groups) showed weight loss above 375 °C in nitrogen, indicative of good thermal stability. Thermally induced phase transition behavior of the polymers was also investigated with differential scanning calorimetry (DSC) in a nitrogen atmosphere. The DSC data are also shown in Table 1. Most of the copolymers had a higher glass transition temperature ( $T_g$ ) than that of the homopolymer, 9,9-dihexylfluorene, which showed a  $T_g$  of about 103 °C in our experiment. Especially for **P9**, it had a  $T_g$  as high as 213 °C. The relatively high glass transition temperatures are essential for many applications, such as emissive materials in light-emitting diodes.<sup>42</sup>

**Optical Properties.** The spectroscopic properties of **P1–P10** were measured both in solution ( $\text{CHCl}_3$ ) and in thin films. The optical properties of **P1–P10** are summarized in Table 2. The representative UV–vis absorption and photoluminescence (PL) spectra for **P2–P6** (of the same main chain structure polyfluorene-*co*-

*alt*-phenylene) in chloroform (ca.  $1 \times 10^{-5}$  M) are shown in Figure 1 and those of **P1** and **P7–P9** (of different main chain structures) are shown in Figure 2. **P2** exhibited the absorption maximum at 369.5 nm. Its PL spectrum peaked at 408 nm, with small shoulders around 431 and 465 nm. In general, the presence of well-defined vibronic structures in the emission spectra indicates that the polymer has a rigid and well-defined backbone structure.<sup>43,44</sup> Because of the electronic effect and less steric hindrance, the absorption spectra of the alkoxy-substituted polymer (**P4**) peaked at 370.5 nm, which was obviously red shifted as compared to the corresponding alkyl-substituted polymer (**P3**). Similar trends were also observed in the emission spectra of these two polymers. In comparison with that of **P2**, the steric hindrance of the alkyl groups in **P3** had caused a blue shift for both the absorption and emission spectra while an obvious red shift was observed for **P4**. When electron-withdrawing groups, such as cyano (**P5**) and ester groups (**P6**), were introduced into the polymer main chain, an obvious blue shift (by 3.5 nm for **P5** and 16.5 nm for **P6**) could be observed in the absorption spectra as compared with that of **P2**. This was attributed to the decrement of electron density in the backbone of polymer induced by the electron-withdrawing effect of the substituted groups. As for the emission spectra, however, both **P5** and **P6** exhibited a red shift

(42) Tokito, S.; Tanaka, H.; Noda, K.; Okada, A.; Taga, Y. *Appl. Phys. Lett.* **1997**, *70*, 1929.

(43) Braun, D.; Heeger, A. J. *Appl. Phys. Lett.* **1991**, *58*, 1982.  
(44) Cimrova, V.; Remmers, M.; Neher, D.; Wegner, G. *Adv. Mater.* **1996**, *8*, 146.

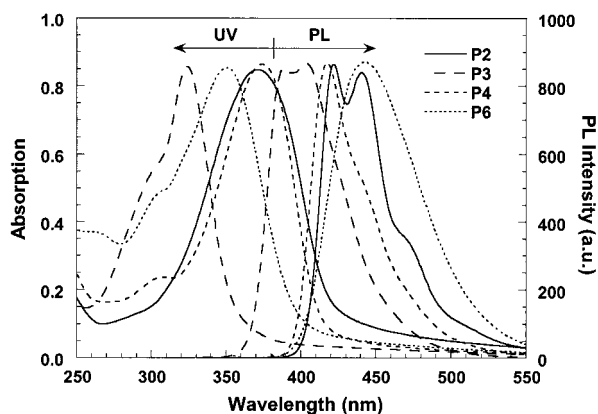


**Figure 3.** UV-visible absorption spectra and photoluminescence spectra of **P2–P4** and **P6** measured from the spin-coated films on quartz plates at room temperature.

with respect to **P2** (by 1.5 nm for **P5** and 43 nm for **P6**), which corresponded to larger Stock's shifts for **P5** and **P6**. Especially for **P6**, the peak difference between absorption and emission spectra was as large as 98 nm, being almost twice those for **P1–P5**. It was also noticed that **P6** exhibited a much broader emission spectrum compared with **P1–P5**. These results implied that the attachment of ester groups enhanced the displacement of the equilibrium geometry of the polymer at the excited states from its ground state.

As depicted in Figure 2, when excited at 379 nm, **P1** showed the fluorescence with a maximum at 415 nm and shoulders at 438 and 469 nm, respectively. **P2** gave similar absorption and emission spectra to **P1**, with a slight blue shift. When the carbazole moiety was copolymerized into the polymer main chain, both the absorption and the emission spectra showed an obvious blue shift as compared to those of the homopolymer **P1**. This phenomenon can be explained that, in **P7**, the coplanarity between the adjacent fluorene and carbazole moiety is poorer than that between the two fluorene rings in **P1** because of the linkage manner via the 3,6-position for the carbazole moiety in **P7**. In **P8**, the contradictory effects of the electropositive and flexible properties of the thiophene ring and the steric effect of the two alkyl groups on the thiophene ring caused the absorption spectrum to be slightly blue shifted by 12 nm in comparison to that with **P1**, with the maximum at 367 nm, while the main peak of the PL spectrum occurred at 447 nm, with a small shoulder at 473 nm, which was red shifted about 32 nm as compared to that of **P1**. The obvious blue shift in the absorption spectrum of **P9** (as compared with that of **P1**) could be understood in terms of the enhanced steric effect of the naphthalene group, which increases the torsion angle between the fluorene and naphthalene units and thus reduces the effective conjugation length along the polymer main chain, leading to the blue shift. As for **P10**, when pyridine was chosen as the comonomer, both the absorption and emission spectra had shown a slight red shift in comparison with those of **P1**.

Transparent and uniform films of all the polymers were prepared on quartz plates by spin-casting their solutions in toluene at room temperature. All 10 polymers emitted blue light under the UV excitation in the solid states. The representative UV-visible and PL

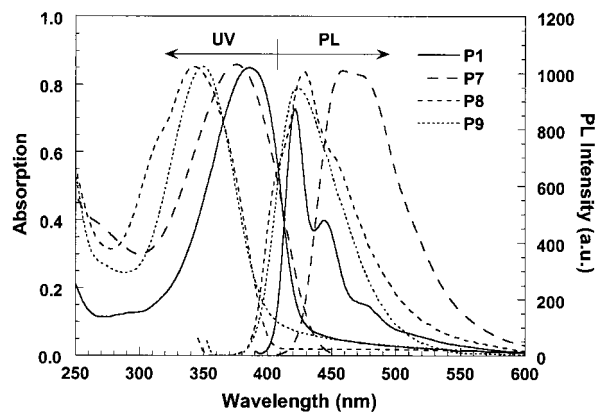


**Figure 4.** UV-vis absorption spectra and photoluminescence spectra of **P1** and **P7–P9** measured from the spin-coated films on quartz plates at room temperature.

spectra of **P2–P6** and **P1**, **P2**, and **P7–P10** as films are displayed in Figures 3 and 4, respectively. Except for **P6** and **P8**, both the absorption spectra and the PL spectra of the other eight polymers were only slightly red shifted with respect to their corresponding spectra in solution, an indication that there were no noticeable molecular conformation changes from solution to the solid states. However, it was strange to find that, for **P6**, there was a slight blue shift between both the absorption and emission spectra in its solution and film states. For **P8**, in contrast to its similar absorption between the solution and the film states, the main emission peak in the solid states shifted about 30 nm toward the longer wavelength in comparison with its solution emission at 398 nm. This may be due to a better conjugation along the polymer main chain in the solid state or the intrachain and/or interchain mobility of the excitons and excimers generated in the solid state of the polymer. It was found that, for **P4**, **P5**, and **P6**, the vibronic structures in the emission were dramatically reduced as compared to those for **P2**, which means that suitable side chains modification can enhance the amorphousness of the resulting polymers in the solid states. The spectroscopic parameters of the polymers are summarized in Table 2.

The fluorescence quantum yields ( $\Phi_f$ ) of the polymers both as films and in chloroform solutions were estimated by using 9,10-diphenylanthracene (dispersed in PMMA films with a concentration lower than  $1 \times 10^{-3}$  M, assuming a PL efficiency of 83%) and quinine sulfate (ca.  $1 \times 10^{-5}$  M solution in 0.1 M  $\text{H}_2\text{SO}_4$ , having the fluorescence quantum yield of 55%) as standards.<sup>45</sup> The results are listed in Table 2. It was found that the polymers with the main chain structure of polyfluorene-*co-alt*-phenylene had higher  $\Phi_f$  values (both in films and in solution) than those with other main chain structures. However, it is worth noting that the presence of the carbonyl function in **P6** reduces strongly the fluorescence quantum yields.

**Electrochemical Properties.** The electrochemical behavior of the polymers was investigated by cyclic voltammetry (CV). CV was performed in a solution of  $\text{Bu}_4\text{NClO}_4$  (0.10 M) in acetonitrile at a scan rate of

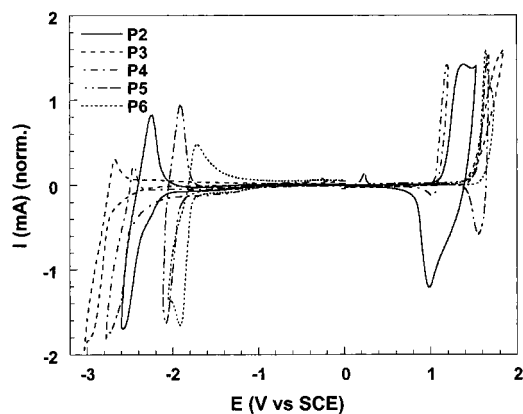
(45) Joshi, H. S.; Jamshidi, R.; Tor, Y. *Angew. Chem., Int. Ed.* **1999**, *38*, 2722.



Table 3. Electrochemical Properties of P1–P10

polymer	<i>n</i> -doping (V) <sup>a</sup>			<i>p</i> -doping (V) <sup>a</sup>			energy levels		
	<i>E</i> <sub>onset</sub>	<i>E</i> <sub>pc</sub>	<i>E</i> <sub>pa</sub>	<i>E</i> <sub>onset</sub>	<i>E</i> <sub>pa</sub>	<i>E</i> <sub>pc</sub>	HOMO	LUMO	<i>E</i> <sub>g</sub> (eV) <sup>b</sup>
<b>P1</b>	-2.03	-2.62	-2.16	1.10	1.59	1.10	5.50	2.37	3.13
<b>P2</b>	-1.93	-2.56	-2.20	0.96	1.40	0.97	5.36	2.47	2.89
<b>P3</b>	-2.09	-2.94	-2.70	1.26	1.80		5.66	2.31	3.35
<b>P4</b>	-1.99	-2.76	-2.45	0.98	1.17	1.05	5.38	2.41	2.97
<b>P5</b>	-1.59	-2.07	-1.91	1.38	1.68	1.56	5.78	2.81	2.97
<b>P6</b>	-1.60	-1.93	-1.72	1.36	1.64	1.20	5.76	2.80	2.96
<b>P7</b>	-1.75	-2.48	-2.23	1.13	1.49	1.18	5.53	2.65	2.88
<b>P8</b>	-1.93	-2.74		0.88	1.21	0.88	5.28	2.47	2.81
<b>P9</b>	-1.98	-2.65	-2.23	1.24	1.69	1.23	5.64	2.42	3.22
<b>P10</b>	-1.57	-2.13	-1.99	1.29	1.55	1.37	5.69	2.83	2.86

<sup>a</sup> *E*<sub>pa</sub> and *E*<sub>pc</sub> stand for anodic peak potential and cathodic peak potential, respectively. <sup>b</sup> *E*<sub>g</sub> stands for the band gap energy.



**Figure 5.** Cyclic voltammograms of **P2–P6** films coated on platinum plate electrodes in acetonitrile containing 0.1 M Bu<sub>4</sub>NClO<sub>4</sub>. Counter electrode: platinum wire. Reference electrode: Ag/AgNO<sub>3</sub> (0.10 M in acetonitrile). Scan rate: 50 mV/s.

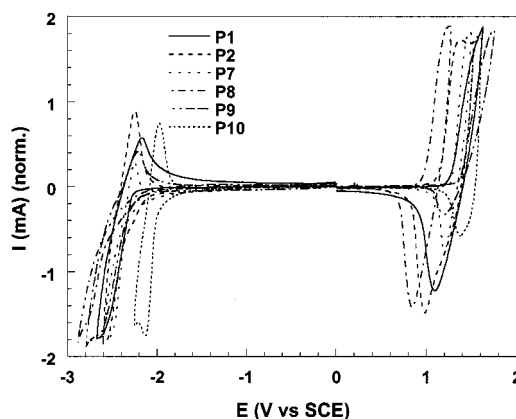


**Figure 6.** Cyclic voltammograms of **P1, P2, and P7–P10** films coated on platinum plate electrodes in acetonitrile containing 0.1 M Bu<sub>4</sub>NClO<sub>4</sub>. Counter electrode: platinum wire. Reference electrode: Ag/AgNO<sub>3</sub> (0.10 M in acetonitrile). Scan rate: 50 mV/s.

50 mV/s at room temperature under the protection of argon. A platinum electrode ( $\approx 0.08$  cm<sup>2</sup>) coated with a thin polymer film was used as the working electrode. A Pt wire was used as the counter electrode and an Ag/AgNO<sub>3</sub> electrode was used as the reference electrode. The corresponding data are summarized in Table 3.

As shown by the cyclic voltammograms in Figure 5 (comparison among the same main chain structures with different side chains **P2–P6**) and 6 (comparison among main chain structures **P1, P2, and P7–P10**), all polymers except **P6** and **P8** exhibited partial reversibility in both *n*-doping and *p*-doping processes. As depicted in Figure 5, the polymers **P2–P6** had the same backbone structure of poly(fluorene-*co-alt*-phenylene) with the difference lying in the fact that protons at the 2- and 5-positions of the phenylene ring had been substituted by different functional groups. When the phenylene ring was substituted by alkyl groups (**P3**), the band gap was enlarged to 3.35 eV because of the steric effect, which agreed with the obvious spectral blue shift as compared to those of **P2** and **P4**. When the strong electron-donating alkoxy group was introduced into the benzene ring, the oxidation and reduction peaks of **P4** located at 1.11 and  $-2.60$  V, respectively, with a band gap of 2.97 eV. When electron-withdrawing groups, such as cyano (**P5**) and ester (**P6**) groups, were attached to the phenylene ring, the band gap energies were still close to those of **P2** and **P4**. However, both the highest occupied molecular orbital (HOMO) and the lowest unoccupied molecular orbital (LUMO) energies had

shifted to a lower energy level. For **P6**, an ester-substituted polymer, the oxidation and the reduction peak potentials were 1.42 and  $-1.83$  V, respectively. It was obvious that it was much easier to reduce **P6** but more difficult to oxidize it, in comparison to **P4**. The oxidation and reduction onset potentials of **P4** were determined to be 0.98 and  $-1.99$  V, from which the HOMO and LUMO energy levels could be estimated as  $-5.38$  and  $-2.41$  eV, respectively. In the same manner, the HOMO and LUMO of **P6** could be determined as  $-5.76$  and  $-2.80$  eV. The obvious difference had well illustrated the adjustable HOMO and LUMO energy levels via side chain modification.

The electronic properties of polyfluorene homopolymer and its copolymers of different main chain structures were also studied. The cyclic voltammograms are shown in Figure 6. For the homopolymer **P1**, we might find that upon cathodic sweeping of the polymer, the onset of the reduction occurred at  $-2.03$  V, with a cathodic peak at  $-2.62$  V and a corresponding reoxidation peak at  $-2.16$  V. The *n*-doping potential  $E_{\text{red}}^{1/2}$  was thus calculated to be  $-2.39$  V. In the anodic scan, the oxidation (*p*-doping) process gave a sharp peak at 1.59 V with the re-reduction peak appearing at 1.10 V. Accordingly, the *p*-doping potential  $E_{\text{ox}}^{1/2}$  was determined to be 1.34 V, and the HOMO and LUMO energy levels were estimated to be  $-5.50$  eV and  $-2.37$  eV, respectively. The electrochemical properties of **P2** and **P1** were quite similar, with a slightly smaller band gap (by 0.24 eV) in **P2** than in **P1**. As for **P7**, by insertion

of the thiophene unit, which is a strong  $\pi$ -excessive group, into the polymer main chain, a decrease in the oxidation potential was expected initially. However, probably because of the decrease in effective conjugation of the polymer main chain caused by the steric hindrance of the two alkyl groups on the thiophene ring, **P7** showed almost the same oxidation peak potential as that of **P1**. On the other hand, there was an obvious difference in the onset potential of the *n*-doping process between the two polymers, which caused a decrement of 0.3 eV of LUMO energy level for **P7** when compared to **P1**. A comparison of the electrochemical data of **P8** with those of **P1** could find an obvious decrease in the oxidative onset potential and a slight increase in the oxidative onset potential for **P8**, and consequently, an increased HOMO and a decreased LUMO energy level as compared to those for **P1**. This revealed that because of the addition of the electron-rich carbazole moiety, **P8** was more electropositive than **P1**. As for **P9**, mainly due to less conjugation along the polymer main chain, it exhibited a higher *p*-doping peak potential (by  $\approx 0.28$  eV) and a slightly larger band gap compared to those of **P2**. For **P10**, which had an electron-deficient moiety, pyridine, in its main chain structure, both the reduction and oxidation potentials had obviously increased when compared to those of **P1**, and consequently both the HOMO ( $-5.69$  eV) and LUMO ( $-2.83$  eV) energy levels were noticeably lowered. These results, once again, demonstrated that both the HOMO and LUMO energy levels of the polyfluorene copolymers could be easily

adjusted in the range of 0.3–0.5 eV by verifying the comonomers while the blue emission of the polymers is maintained.

### Conclusions

Ten polyfluorene copolymers composed of alternating 9,9-dihexylfluorene with different main chain structures and those of the same main chain structure polyfluorene-*co-alt*-phenylene with different functional groups attached at the 2- and/or 5-positions of the phenylene ring had been synthesized by palladium-catalyzed Suzuki coupling reactions. Efficient blue light emission, good solubility in common organic solvents, good thermal stability, and relatively high glass transition temperatures had been demonstrated in all 10 polymers. The optical, electrochemical, and thermal properties all exhibited dependence on the changes in main chain structures as well as the side chain groups attached on the phenylene ring. The band gaps of 10 polymers were varied between 2.81 and 3.35 eV. Modification of the main chain and related side chain with a variety of electron-withdrawing or electron-donating groups enabled the tuning of HOMO and LUMO energy levels in the range of 0.4–0.5 eV for the blue-light-emitting polymers. Such a wide tuning of molecular orbital energy levels in blue-light-emitting polymers is meaningful for the fabrication of efficient blue-light-emitting devices.

CM0007048